Mine Water and the Environment (2020) 39:112–120
https://doi.org/10.1007/s10230-019-00646-w

TECHNICAL ARTICLE

Estimating the Hydraulic Conductivity of Deep Fractured Rock Strata from High-pressure Injection Tests

Zhen Huang[1,2,3] · Shijie Li[1] · Kui Zhao[1] · Yun Wu[3] · Wei Zeng[1] · Hongwei Xu[1]

Received: 22 October 2018 / Accepted: 1 November 2019 / Published online: 7 November 2019

Abstract

Deep coal mining in the Yanzhou coalfield is threatened by a confined Ordovician limestone aquifer where water pressure exceeds 10 MPa. High-pressure injection tests are widely used to characterize the hydraulic properties of water-resisting fractured rock strata under such conditions, although estimating hydraulic conductivity remains an issue. This paper presents an approach to estimate it, using data from several high-pressure injection tests by accounting for the flow conditions. Typical *P*–*Q* curves obtained from the injection tests were summarized and divided into Darcian and non-Darcian flow phases, and an equation was proposed to estimate the hydraulic conductivity of fractured rocks. The hydraulic conductivity is pressure dependent and increased by injection pressure in the non-Darcian flow phase, due to hydraulic fracturing. As one would expect, the hydraulic conductivity estimated using the new equation was much greater than that estimated using Darcy's law.

Keywords Water inrush · Hydraulic properties · Non-Darcian flow · Hydraulic fracturing

Introduction

Coal remains the primary energy source in China (Ding et al. 2017). China produced an estimated 3.46 billion metric tons (t) and 3.52 billion t of coal output in 2016 and 2017. According to China's National Energy Development Strategy Plan (2014–2020), coal will continue to control China's energy strategy, contributing more than 60% of the country's energy (Zhang et al. 2016). However, coal production in China is always threated by water inrush accidents (e.g. Bai et al. 2013; Bukowski 2011; Huang et al. 2014; Ma et al. 2017; Meng et al. 2012; Zhang and Shen 2004). Water inrush risk rises with increased water pressure and mining depth (Meng et al. 2012). The most serious of the possible water disasters affecting coal production is groundwater inrush from the Ordovician limestone underlying the Permo-Carboniferous coal seams in northern China (Bai et al. 2013; Zhang and Shen 2004). The Ordovician limestone is a confined karst aquifer that contains an abundant supply of water under a hydrostatic pressure that exceeds 10 MPa; however, the strata between the coal seams and this aquifer, which act as barrier to groundwater inrush, are relatively thin in these coalfields (Bai et al. 2013; Peng and Zhang 2007). The hydraulic conductivity of fractured strata is important for understanding groundwater flow and transport phenomena in a rock aquifer system (Chen et al. 2015) and for investigating the risk of water inrush (Huang et al. 2018; Zhu and Zhang 2018). In addition, other applications ranging from oil production to high-head pumped-storage power stations and underground engineering have an increasing requirement for the hydraulic conductivity of rock strata (Angulo et al. 2011; Huang et al. 2016; Zhou et al. 2018).

In-situ pumping or injection tests are considered to be a reliable technique for investigating the hydraulic properties of rocks in field conditions (Chen et al. 2015; Hamm et al. 2007; Huang et al. 2016, 2018; Neuman 2005; Zhu and Zhang 2018). Conventional hydraulic tests are typically performed at low injection pressures (≤ 1 MPa) or low flow rates, which are inappropriate for deep environments with high water pressure (Chen et al. 2015; Huang et al. 2018;

✉ Zhen Huang
huangzhen@nju.edu.cn; zhenhuang89@126.com

✉ Kui Zhao
kzjxlg@163.com

[1] School of Resources and Environment Engineering, Jiangxi University of Science and Technology, Ganzhou 341000, China

[2] State Key Laboratory for GeoMechanics and Deep Underground Engineering, Xuzhou 221116, China

[3] School of Earth Sciences and Engineering, Nanjing University, Nanjing 210023, China

Zhou et al. 2018). High-pressure injection tests are commonly used to investigate the hydraulic properties of rock formations under high water pressure in a deep environment (Cappa et al. 2006; Chen et al. 2015; Cornet et al. 2003; Derode et al. 2013; Huang et al. 2014, 2016, 2018; Rutqvist et al. 1998; Zhou et al. 2018), where the maximum injection pressure is higher than 1 MPa. This high water pressure and hydraulic gradient can produce a transition to nonlinear flow, due to high flow velocities in fractures (Chen et al. 2015; Huang et al. 2018; Zhou et al. 2015, 2018; Zimmerman and Bodvarsson 1996). Darcy's law-based methods are often used to estimate hydraulic conductivity, due to their ease of implementation and computational efficiency (e.g. Hamm et al. 2007; Huang et al. 2014, 2016, 2018; Lo et al. 2014; Neuman 2005; Rutqvist et al. 1998; Zhu and Zhang 2018), ignoring the nature of nonlinear flow in fractured rocks at high flow rates or hydraulic gradients (Chen et al. 2015; Zhou et al. 2018). Some methods have been proposed in recent years for non-Darcian flow conditions, although only a few of them targeted or are suitable for high-pressure injection tests (Chen et al. 2015; Yamada et al. 2005; Zhou et al. 2018). There is a need for an appropriate method to calculate the hydraulic conductivity from high-pressure injection test data. In this paper, we present an approach to do this, using published data from several high-pressure injection tests. The permeability variations in the fractured strata between the deep coal seams and Ordovician limestone aquifer are discussed.

Geological and Hydrogeological Setting

The Yanzhou coalfield is located in Jining city, in western Shandong, China (Fig. 1a). The deep coal seams in the Yanzhou coalfield, i.e. the no. 16 bottom coal and no. 17 coal seams, have been or will be mined due to the gradual

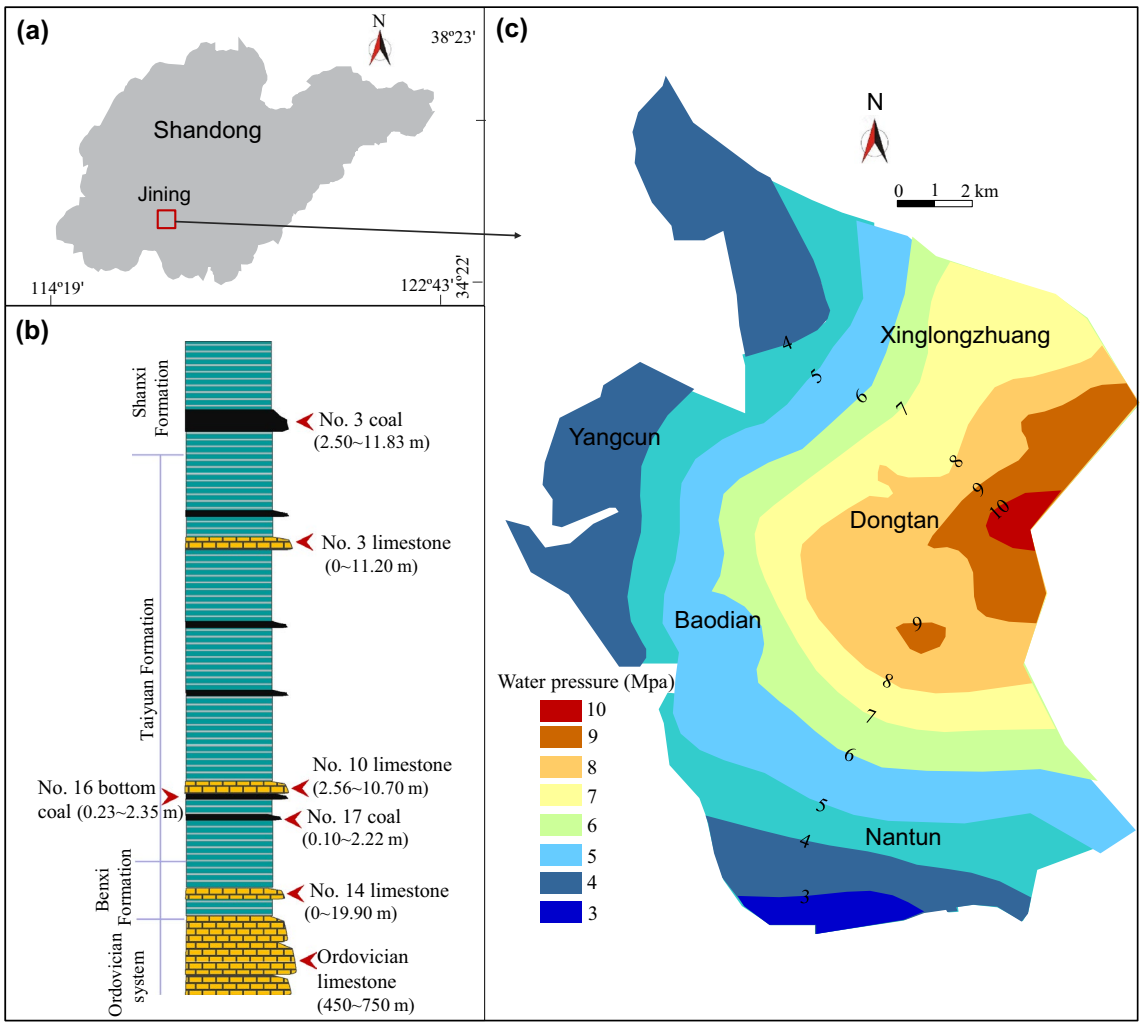

Fig. 1 **a** The study area location, **b** the geological column of the Yanzhou coalfield, and **c** the contours of water pressure of the Ordovician limestone aquifer in the Yanzhou coalfield

depletion of shallow coal resources. The thicknesses of these two coal seams range from 0.23 to 2.35 m (no. 16) and from 0.1 to 2.22 m (no. 17). The total coal reserves of the two seams are estimated at 5.77 million t. As shown in Fig. 1b, these two seams both lie at the bottom of the Taiyuan Formation, and may be hydraulically connected with the underlying no. 14 limestone and Ordovician limestone (Liang et al. 2015). The Ordovician limestone, located below the deep coal seams, is a highly permeable confined aquifer (Liang et al. 2015) that is 450–750 m thick. Water pressure in the Ordovician limestone aquifer can be high as 3–10 MPa (Fig. 1c), which poses a great challenge to coal production. Moreover, the thickness of the aquifuge (i.e. the rock formations between the coal seams and the Ordovician limestone aquifer) is thin, ranging from 40 to 80 m. Thus, the Ordovician limestone aquifer significantly influences mining of the deep coal seams in this area. We need to better determine the area's hydrogeological parameters, particularly the hydraulic conductivity of the strata, to determine the risk of water inrush.

Characteristics of Flow Patterns in the High-pressure Injection Tests

Data from high-pressure injection tests are generally plotted on a graph that shows the pressure and injection rate as a function of time. The relationship between the injection pressure (P) and the injection rate (Q) are shown in the form of P-Q curves, which account for the flow behavior in fractured strata under increasing injection fluid pressure (Chen et al. 2015; Huang et al. 2014, 2018; Quinn et al. 2011; Rutqvist et al. 1998; Zhou et al. 2018). The injection pressure is the column of water in the tested intervals plus the pressure exerted by the injection device. Figure 2 presents an example of the test results and its P–Q curve for a high-pressure injection test performed in the mudstone under the deep coal seams of the Dongtan coal mine (Huang et al. 2015, 2018, 2019). The P–Q curves obtained from the high-pressure injection tests are typically nonlinear due to the deviation from linear flow or the occurrence of fracture dilation and/or hydraulic fracturing in the rocks (Chen et al. 2015; Huang et al. 2018, 2019; Zhou et al. 2018). The P–Q curves for the high-pressure injection tests are generally divided into two phases using the turning point (Q_c, P_c) (Chen et al. 2015; Huang et al. 2014, 2018; Zhou et al. 2018), as shown in Fig. 3. In phase I, the P–Q curve is an apparent linearity that extrapolates through the origin when the injection fluid pressure P is less than the critical fluid pressure P_c, indicating that the flow in the rock follows Darcy's law and is considered Darcian flow (Huang et al. 2018, 2019). In phase II, the increased injection pressure ($P > P_c$) causes remarkable fracture dilation and hydraulic fracturing,

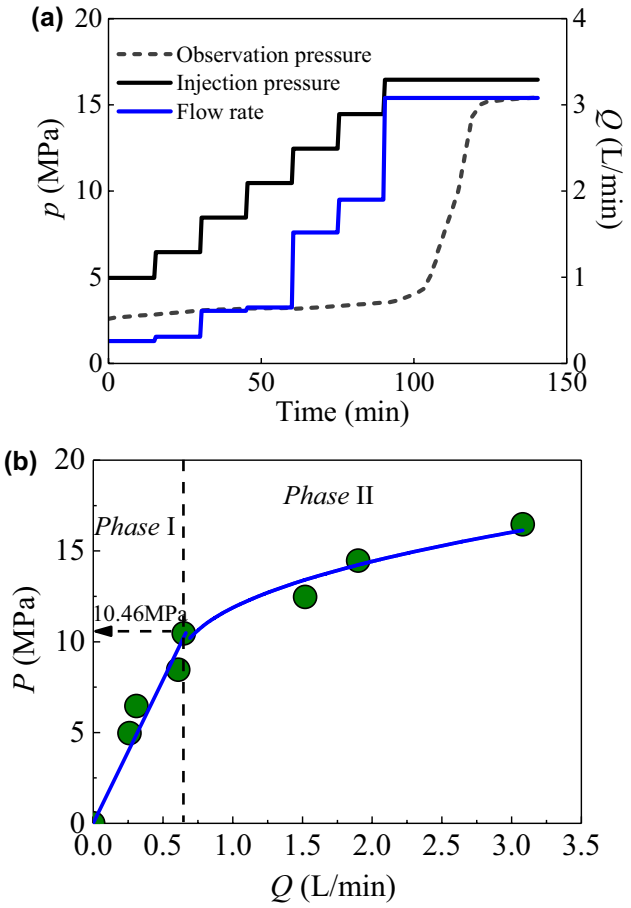

Fig. 2 The raw data of a typical high-pressure injection test. **a** Temporal evolution of injection pressure, observation pressure, and injection rate; **b** P–Q curve (after Huang et al. 2015, 2018, 2019)

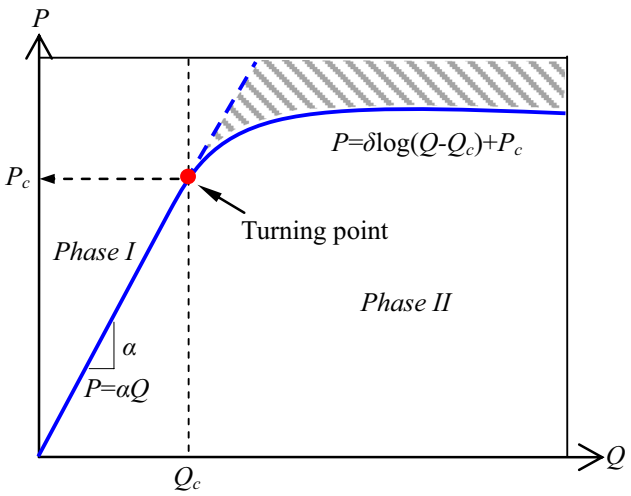

Fig. 3 A conceptual model of the P–Q curves obtained from the high-pressure injection tests

which results in the flow becoming nonlinear (Chen et al. 2015; Huang et al. 2014, 2018, 2019; Zhou et al. 2018). The fluid flow in fractured rocks induced by high-pressure injections is typically partitioned into two phases, i.e. the Darcian (Phase I) and the non-Darcian flow phase (Phase II). The *P*–*Q* curves for the high-pressure injection tests have been described by Huang et al. (2018):

$$P = \begin{cases} \alpha_{\mathrm{I}} Q \ (0 < P \le P_c) & \text{(Phase I)} \\ \alpha_{\mathrm{II}} (Q - Q_c)^{\beta} + P_c \ (P > P_c) & \text{(Phase II)} \end{cases} \tag{1}$$

where α_{I}, α_{II} and β are fitting coefficients, P_c is critical injection pressure that initiates hydraulic fracturing, and Q_c is the corresponding injection rate.

Discussion

Mathematical Model of Hydraulic Conductivity

Hydraulic conductivity (k) is an important parameter for characterizing hydraulic properties and the connectivity of fractured rocks that can be estimated from the results of the in situ hydraulic tests (e.g. Angulo et al. 2011; Chen et al. 2015; Fernandez and Moon 2010; Huang et al. 2014, 2016, 2018; Zhou et al. 2018). Hydraulic conductivity is commonly estimated assuming a steady-state laminar flow in a homogeneous and isotropic media surrounding a test borehole or well (e.g., Angulo et al. 2011; Hamm et al. 2007; Huang et al. 2014, 2016, 2018). The Darcy's law-based equation is usually applied (Hvorslev 1951):

$$k = \frac{Q}{2\pi L H_0} \ln\left[\frac{L}{2r_w} + \sqrt{1 + \left(\frac{L}{2r_w}\right)^2}\right] \tag{2}$$

where k is the hydraulic conductivity, Q is the flow rate, r_w is the radius of the borehole, L is the length of the test section, and H_0 is the water head difference. If L/r_w is higher than 10, Eq. 2 is reduced to (Angulo et al. 2011)

$$k = \frac{Q}{2\pi L H_0} \ln\left(\frac{L}{r_w}\right) \tag{3}$$

The findings from the high-pressure fluid injection tests performed in the fractured rocks under the deep coal seams of the Yanzhou coalfield show that there are two distinct flow regimes (Huang et al. 2014, 2016, 2018), and that the flow rate within the fractures induced by high fluid pressure is greater than at low pressure (Chen et al. 2015; Meng et al. 2014; Zhou et al. 2018). The classical Darcy's law-based equations for estimating hydraulic conductivity (Chen et al. 2015; Zhou et al. 2018), e.g. Eqs. 2 and 3, are inadequate for turbulent flow conditions non-Darcian flow (phase II).

If the fracture density is low or the fracture system is highly anisotropic, a one- or two-dimensional model would be preferable (Barker 1988). Jiang et al. (2007) predicted that hydraulic fracturing occurs in homogeneous and isotropic media, forming numerous flow circles and fracturing circles surrounding the injection borehole. We assume that: (1) the test rocks are homogeneous and isotropic; (2) at any given point ζ on the interval, the volumetric flow rate dq injected into the infinitesimal section $d\zeta$ is linearly proportional to the total volumetric flow rate Q injected into the test interval L (Chen et al. 2015; Meng et al. 2014; Rutqvist et al. 1998). Thus, at any flow circle corresponding to a given point (r, θ) surrounding the injection borehole, the volumetric flow rate Q_r injected into the circle is equal to the total volumetric flow rate Q (Jiang et al. 2007, 2010), as shown in Fig. 4. The Forchheimer equation ($i = av + bv^2$) (Forchheimer 1901) and the Izbash equation ($v = ki^{1/m}$) (Izbash and Leleeva 1971) are proposed for non-Darcian flow in homogeneous and isotropic aquifers (Chen et al. 2015), as it is recognized that the phase II flow is non-Darcian, where i is hydraulic gradient, v is volumetric flow velocity, and a, b, and m are empirical coefficients).

The Izbash equation was used, so the total volumetric flow rate Q and the volumetric flow rate Q_r injected into the circle at any flow circle corresponding to a given point (r, θ) are expressed as:

$$\begin{cases} Q = 2\pi r_w v_0 L = 2\pi r_w k i_0^{1/m} L \\ Q_r = 2\pi r v_r L = 2\pi r k i_r^{1/m} L \\ Q = Q_r \end{cases} \tag{4}$$

where v_0 and v_r is volumetric flow velocity at the injection borehole and the point (r, θ), and i_0 and i_r are the hydraulic gradients corresponding to v_0 and v_r. The relationship between i_0 and i_r is written as:

$$i_r = \left(\frac{r_w}{r}\right)^m i_0 \tag{5}$$

At any flow circle corresponding to the given point (r, θ) surrounding the injection borehole, the water head increment is expressed as (Jiang et al. 2010)

$$dp = i_r dr \tag{6}$$

Integration of both sides of Eq. 6 provides:

$$\int_0^{p_0} dp = \int_{r_w}^{L_e} i_r dr \tag{7}$$

Based on Eq. 5, we have:

$$\int_0^{p_0} dp = \int_{r_w}^{L_e} \left(\frac{r_w}{r}\right)^m i_0 dr \tag{8}$$

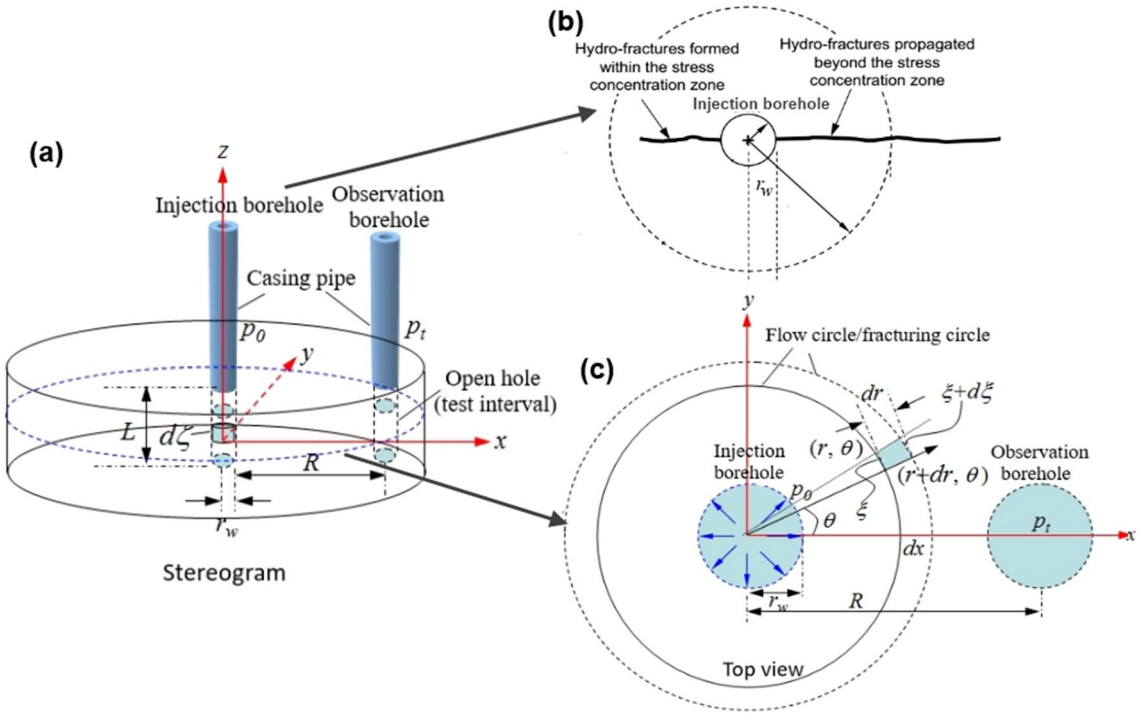

Fig. 4 Conceptual model for the formula derivation of hydraulic conductivity. **a** Stereogram of the high-pressure fluid injection test, **b** hydro-fractures propagation geometry around the injection borehole (Lee and Ong 2018), and **c** sketch of fluid flow in the test interval (modified from Huang et al. 2014)

$$p_0 = \frac{i_0 r_w^m}{m-1}\left(\frac{1}{r_w^{m-1}} - \frac{1}{L_e^{m-1}}\right) \tag{9}$$

$$i_0 = \frac{(m-1)p_0 L_e^{m-1}}{r_w(L_e^{m-1} - r_w^{m-1})} \tag{10}$$

where p_0 is understood as the pressure head in the injection borehole, and L_e is the radius of influence by fluid injection. Substituting Eq. 10 into Eq. 4:

$$Q = 2\pi k L r_w L_e^{\frac{m-1}{m}}\left[\frac{(m-1)p_0}{r_w L_e^{m-1} - r_w^m}\right]^{1/m} \tag{11}$$

The hydraulic conductivity k in Phase II is calculated by:

$$k = \frac{Q}{2\pi\left[(m-1)p_0\right]^{1/m} L}\left[\left(\frac{L_e}{r_w}\right)^{m-1} - 1\right]^{1/m} L_e^{\frac{m}{m-1}} \tag{12}$$

For $m=2$, i.e. the flow is turbulent (Chen et al. 2015), Eq. 12 is rewritten as:

$$k = \frac{Q}{2\pi p_0^{1/2} L}\left[\frac{L_e}{r_w} - 1\right]^{1/2} L_e^2 \tag{13}$$

The hydraulic conductivity is calculated using the data recorded from the injection borehole and observation borehole (Huang et al. 2014, 2016, 2018). Along the spring line $\theta=0$, we have:

$$i_r = \left(\frac{R}{r}\right)^m i_R \tag{14}$$

where R is the distance from the injection borehole to the observation borehole, i_R the hydraulic gradient at the point $(R, 0)$. Integration of both sides of Eq. 14 gives

$$\int_{p_t}^{p_0} dp = \int_{r_w}^{R} i_r dr \tag{15}$$

where p_t is understood as the pressure head in the observation borehole. We obtain Eq. 16 to estimate the hydraulic conductivity in the Non-Darcy flow phase (phase II) as:

$$k_{\mathrm{II}} = \frac{Q}{2\pi(p_0 - p_t)^{1/2}L}\left[\frac{R}{r_w} - 1\right]^{1/2} R^2 \tag{16}$$

The Darcy's law-based equations (i.e. Eqs. 2 and 3) should still be used to calculate the hydraulic conductivity (k_{I}) due to Darcian flow in the rocks at low injection pressures (phase I).

A Case Study

We studied previously obtained data from high-pressure injection tests performed in six fractured strata between the deep coal seams and the Ordovician limestone aquifer of the Baodian and Dongtan coal mines (Huang et al. 2015, 2018, 2019), and estimated their hydraulic conductivities. These tests took place at depths of 625.8–842.3 m (Table 1). The turning point (Q_c, P_c) was used to characterize the onset of the flow transition to nonlinear, and the critical water pressures from these injection tests are summarized in Table 1.

The Darcian equation, i.e. Eq. 3, was used to estimate the hydraulic conductivity (k_{I}) for $P < P_c$ in phase I, and the non-Darcian equation, i.e. Eq. 16 was used to estimate the hydraulic conductivity (k_{II}) for $P > P_c$ in phase II. Table 1 lists the estimated values of the hydraulic conductivities (k_{I} and k_{II}) in the two phases of high-pressure fluid injection tests in the six fractured rocks, where k_{II} is the maximum estimated value. Figure 5 presents the k_{I} and k_{II} vs. the changing injection pressures, i.e. the *P*–*k* curves. Figure 5 demonstrates that in phase I, k_{I} was approximated with a constant and was considered the initial hydraulic conductivity of the test rocks, which is consistent with the conclusions reached by Huang et al. (2014, 2016, 2018) and Chen et al. (2015). The initial hydraulic conductivities of the six fractured rocks range in 3.6×10^{-8} to 6.5×10^{-7} cm/s (Table 1). In agreement with Chen et al. (2015), the hydraulic conductivity mainly depends on natural fractures within the rocks and the physical properties of the fluid in phase I, which is constant as long as the injection pressure is low enough to avoid fracture dilation and hydraulic fracturing.

When the injection pressure reaches the threshold fluid pressure P_c, the hydraulic conductivity becomes pressure dependent and increases with the injection pressure (Fig. 5), due to tensile cracking and fracture dilation induced by hydraulic fracturing (Chen et al. 2015; Guglielmi et al. 2015). The results show the magnitude of the hydraulic conductivity increases several times in phase II, ranging between 1846-fold to 105,491-fold increase (Table 1). The estimated hydraulic conductivity $k_{\mathrm{II}}^{'}$ using the non-Darcian flow equation is typically 480–4250 times larger than the estimated hydraulic conductivity k_{II} using the Darcian flow equation. These permeability increases are probably due to hydraulic fractures, based on hydraulic fracturing experiments on rock cores (He et al. 2017), as shown in Fig. 6. The hydraulic conductivity of the fractures induced by hydraulic fracturing is greater than that of the rock matrix.

The above estimates of hydraulic conductivity in this study have uncertainties (Chen et al. 2015), but our calculated method and results could be widely used to characterize the hydraulic properties of fractured rocks in many applications, from coal and oil production to high-head pumped-storage power stations (Huang et al. 2016; Zhou et al. 2018).

Table 1 Hydraulic conductivity estimates from the high-pressure injections test data performed in six fractured rock strata in the Yanzhou coalfield (after Huang et al. 2018)

Coal mine	Media	Depth (m)	k_{I} (cm/s)	k_{II} (cm/s)			$k_{\mathrm{II}}^{'}/k_{\mathrm{I}}$
				k_{II} (using Eq. 3)	$k_{\mathrm{II}}^{'}$ (using Eq. 16)	$k_{\mathrm{II}}^{'}/k_{\mathrm{II}}$	
Baodian	Mudstone/siltstone	625.8–636.3	2.9×10^{-7}	2.3×10^{-6}	1.3×10^{-3}	565	4524
Baodian	Limestone	636.3–645.5	6.5×10^{-7}	3.8×10^{-6}	2.2×10^{-3}	579	1846
Baodian	Mudstone/fine sandstone	645.5–651.2	1.2×10^{-7}	2.5×10^{-6}	2.4×10^{-3}	960	3422
Dongtan	Fine sandstone	756.2–768.3	3.6×10^{-8}	6.4×10^{-8}	7.7×10^{-5}	1203	1921
Dongtan	Mudstone	814.8–824.8	1.1×10^{-7}	2.5×10^{-6}	1.2×10^{-3}	480	19,627
Dongtan	Limestone/mudstone	832.9–842.3	1.4×10^{-7}	4.0×10^{-6}	1.7×10^{-2}	4250	105,491

k_{I} the average estimated initial hydraulic conductivity of the fractured strata using the Darcy's law-based equation (Eq. 3), k_{II} the estimated maximum hydraulic conductivity of the fractured strata using the Darcy's law-based equation (Eq. 3), $k_{\mathrm{II}}^{'}$ the estimated maximum test hydraulic conductivity of the fractured strata using the non-Darcian flow-based equation (Eq. 16)

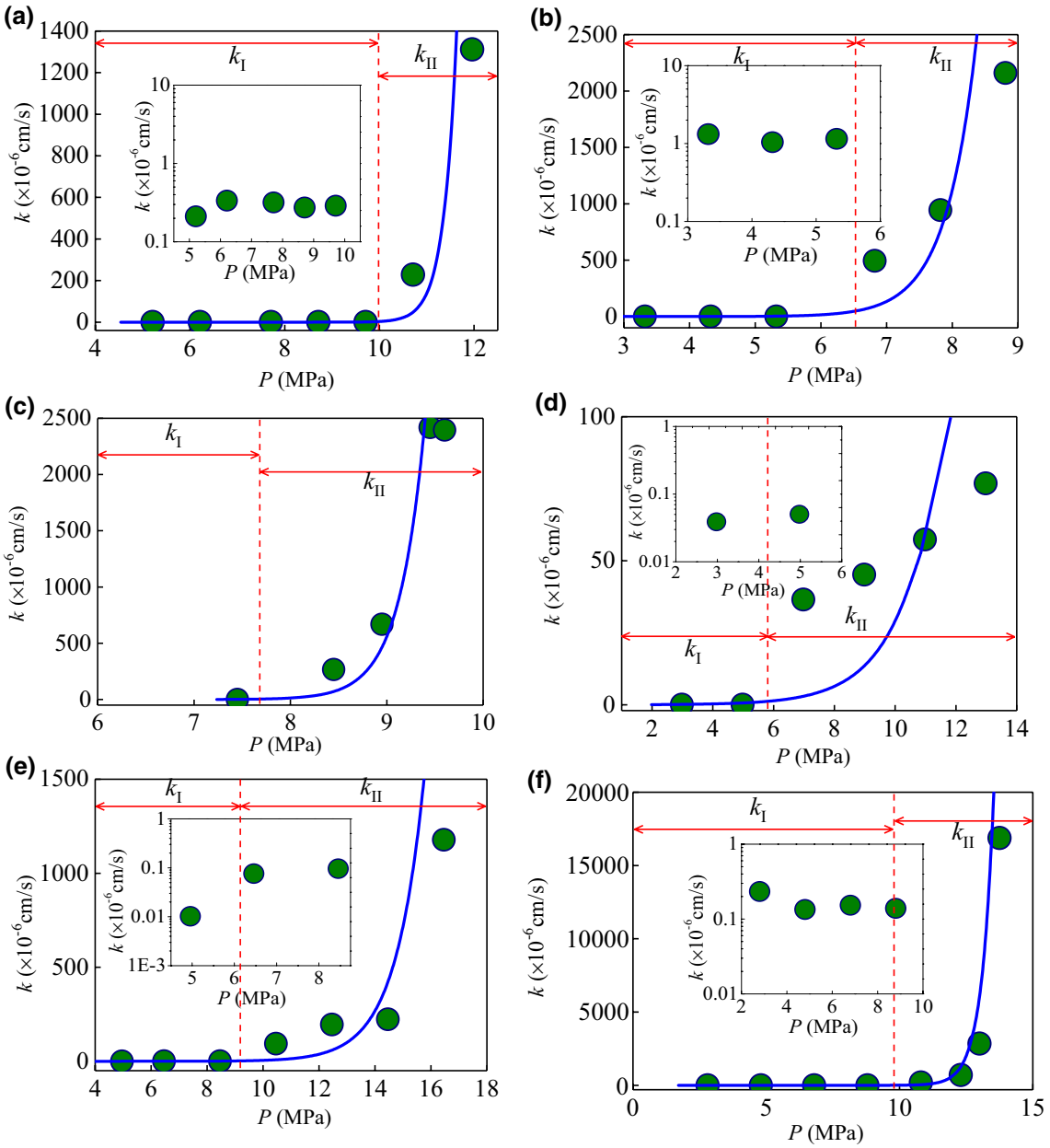

Fig. 5 Estimated hydraulic conductivity vs. injection fluid pressure curves for six fractured rock strata in the Yanzhou coalfield. **a** Mudstone and siltstone, **b** limestone, **c** mudstone and fine sandstone, **d** fine sandstone, **e** mudstone, and **f** limestone and mudstone. Blue lines represent curves fitted to the data points

Conclusions

The Ordovician limestone aquifer's high water pressure poses a great challenge to the production of deep coal seams in the Yanzhou coalfield. High-pressure injection tests are an effective way to investigate the hydraulic properties of fractured water-resisting rock strata under high water pressure conditions, but calculating the hydraulic conductivity from a high-pressure injection test is challenging. In this paper, the flow condition in the fractured strata induced by high water pressure was divided into Darcian and non-Darcian flow phases, based on the characteristics of the obtained *P*–*Q* curves. A non-Darcian flow equation was developed to estimate the hydraulic conductivity of the fractured strata.

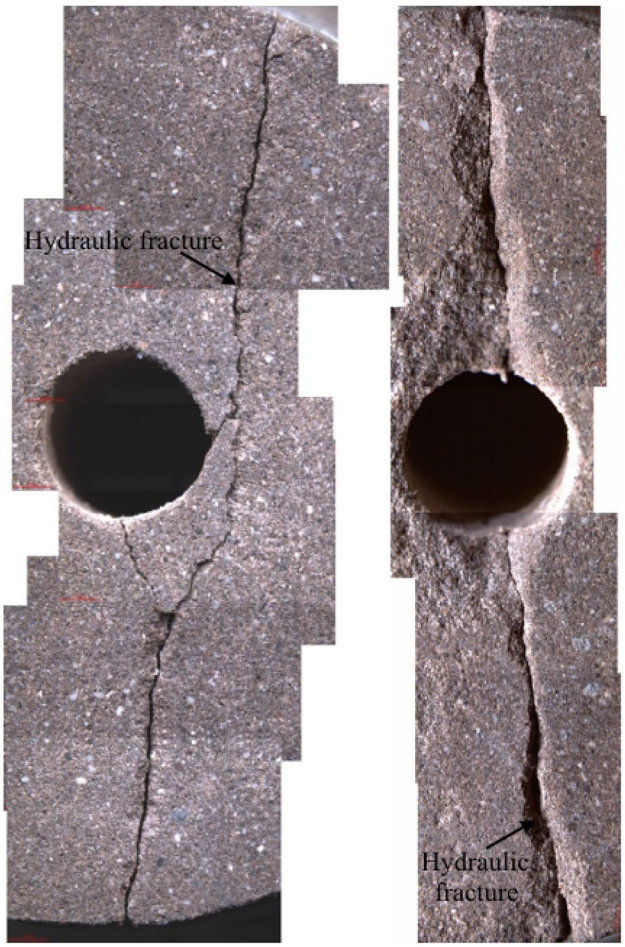

Fig. 6 Symmetrical hydraulic fractures around the injection hole observed by high definition microscope (after He et al. 2017)

The initial hydraulic conductivities of the six fractured rock strata located at depths of 625.76–842.80 m ranged from 3.6×10^{-8} to 6.5×10^{-7} cm/s. The hydraulic conductivity is weakly dependent on the injection pressure during the Darcian flow phase, but becomes strongly pressure dependent in the non-Darcian flow phase, when hydraulic fracturing induced by the high water pressures causes the hydraulic conductivity to increase by several orders of magnitude.

Acknowledgements The authors gratefully thank the editors and anonymous reviewers for their valuable and constructive comments in improving this paper. The authors gratefully acknowledge the financial support from the National Natural Science Foundation of China (41702326), the National Postdoctoral Program for Innovative Talents (BX201700113), the China Postdoctoral Science Foundation (2017M620205), the Natural Science Foundation of Jiangxi Province (20171BAB206022), the State Key Laboratory for GeoMechanics and Deep Underground Engineering, China University of Mining & Technology (SKLGDUEK1703), and the Innovative Experts, Long-term Program of Jiangxi Province (jxsq2018106049).

References

Angulo B, Morales T, Uriarte JA, Antigüedad I (2011) Hydraulic conductivity characterization of a karst recharge area using water injection tests and electrical resistivity logging. Eng Geol 117:90–96

Bai H, Ma D, Chen Z (2013) Mechanical behavior of groundwater seepage in karst collapse pillars. Eng Geol 164:101–106

Barker JA (1988) A generalized radial flow model for hydraulic tests in fractured rock. Water Resour Res 24(10):1796–1804

Bukowski P (2011) Water hazard assessment in active shafts in Upper Silesian coal basin mines. Mine Water Environ 30:302–311

Cappa F, Guglielmi Y, Rutqvist J, Tsang CF, Thoraval A (2006) Hydromechanical modelling of pulse tests that measure fluid pressure and fracture normal displacement at the Coaraze Laboratory site, France. Int J Rock Mech Min Sci 43(7):1062–1082

Chen YF, Hu SH, Hu R, Zhou CB (2015) Estimating hydraulic conductivity of fractured rocks from high-pressure packer tests with an izbash's law-based empirical model. Water Resour Res 51(4):2096–2118

Cornet FH, Doan ML, Fontbonne F (2003) Electrical imaging and hydraulic testing for a complete stress determination. Int J Rock Mech Min Sci 40:1225–1241

Derode B, Cappa F, Guglielmi Y, Rutqvist J (2013) Coupled seismo-hydromechanical monitoring of inelastic effects on injection-induced fracture permeability. Int J Rock Mech Min Sci 61:266–274

Ding L, Dai Z, Guo Q, Yu G (2017) Effects of in situ interactions between steam and coal on pyrolysis and gasification characteristics of pulverized coals and coal water slurry. Appl Energy 187:627–639

Fernandez G, Moon J (2010) Excavation-induced hydraulic conductivity reduction around a tunnel-part 1: guideline for estimate of ground water inflow rate. Tunn Undergr Space Technol 25:560–566

Forchheimer P (1901) Wasserbewegung durch boden. Z Ver Dtsch Ing 45:1782–1788

Guglielmi Y, Cappa F, Avouac J, Henry P, Elsworth D (2015) Seismicity triggered by fluid injection–induced aseismic slip. Science 348:1224–1226

Hamm SY, Kim M, Cheong JY, Kim JY, Son M, Kim TW (2007) Relationship between hydraulic conductivity and fracture properties estimated from packer tests and borehole data in a fractured granite. Eng Geol 92:73–87

He J, Lin C, Li X, Zhang Y, Chen Y (2017) Initiation, propagation, closure and morphology of hydraulic fractures in sandstone cores. Fuel 208:65–70

Huang Z, Jiang Z, Zhu S, Qian Z, Cao D (2014) Characterizing the hydraulic conductivity of rock formations between deep coal and aquifers using injection tests. Int J Rock Mech Min Sci 71:12–18

Huang Z, Jiang Z, Fu J, Cao D (2015) Experimental measurement on the hydraulic conductivity of deep low-permeability rock. Arab J Geosci 8:5389–5396

Huang Z, Jiang ZQ, Zhu SY, Wu XS, Yang LN, Guan YZ (2016) Influence of structure and water pressure on the hydraulic conductivity of the rock mass around underground excavations. Eng Geol 202:74–84

Huang Z, Li X, Li S, Zhao K, Zhang R (2018) Investigation of the hydraulic properties of deep fractured rocks around underground excavations using high-pressure injection tests. Eng Geol 245:180–191

Huang Z, Li X, Li S, Zhao K, Xu H (2019) Variations in hydraulic properties of sedimentary rocks induced by fluid injection: the effect of water pressure. Pol J Environ Stud 28(2):647–655

Hvorslev MJ (1951) Time lag and soil permeability in ground water observations. Waterw. Exp Stn Bull 36, U.S. Army Corps Eng 50, Vicksburg. Mississippi

Izbash SV, Leleeva NM (1971) Aspects of turbulent seepage flow in a fill. Power Tech Eng 5(5):462–465

Jiang Z, Fu S, Li S, Hu D, Feng S (2007) High pressure permeability test on hydraulic tunnel with steep obliquity faults under high pressure. Chin J Rock Mech Eng 26(11):2318–2323

Jiang ZM, Chen SH, Feng SR, Zhang XM (2010) Study on the method for evaluating rock mass permeability coefficient. J Hydraul Eng 41(10):1228–1233

Lee H, Ong SH (2018) Estimation of in situ stresses with hydro-fracturing tests and a statistical method. Rock Mech Rock Eng 51:779–799

Liang DX, Jiang ZQ, Guan YZ (2015) Field research: measuring water pressure resistance in a fault-induced fracture zone. Mine Water Environ 34(3):320–328

Lo HC, Chen PJ, Chou PY, Hsu SM (2014) The combined use of heat-pulse flowmeter logging and packer testing for transmissive fracture recognition. J Appl Geophys 105:248–258

Ma D, Rezania M, Yu HS, Bai HB (2017) Variations of hydraulic properties of granular sandstones during water inrush: effect of small particle migration. Eng Geol 217:61–70

Meng Z, Li G, Xie X (2012) A geological assessment method of floor water inrush risk and its application. Eng Geol 143–144:51–60

Meng R, Hu S, Chen Y, Zhou C (2014) Permeability of non-Darcian flow in fractured rock mass under high seepage pressure. Chin J Rock Mech Eng 33(9):1756–1764

Neuman SP (2005) Trends, prospects and challenges in fractured rock hydrology. Hydrogeol J 13(1):124–147

Peng SP, Zhang JC (2007) Engineering geology for underground rocks. Springer, Berlin

Quinn PM, Cherry JA, Parker BL (2011) Quantification of non-Darcian flow observed during packer testing in fractured sedimentary rock. Water Resour Res 47:W09533. https://doi.org/10.1029/2010WR009681

Rutqvist J, Noorishad J, Tsang C, Stephansson O (1998) Determination of fracture storativity in hard rocks using high-pressure injection testing. Water Resour Res 34(10):2551–2560

Yamada H, Nakamura F, Watanabe Y, Murakami M, Nogami T (2005) Measuring hydraulic permeability in streambed using the packer test. Hydrol Process 19(13):2507–2524

Zhang J, Shen B (2004) Coal mining under aquifers in China: a case study. Int J Rock Mech Min Sci 41:629–639

Zhang Y, Shao W, Zhang M, Li H, Yin S, Xu Y (2016) Analysis 320 coal mine accidents using structural equation modeling with unsafe conditions of the rules and regulations as exogenous variables. Accid Anal Prev 92:189–201

Zhou JQ, Hu SH, Fang S, Chen YF, Zhou CB (2015) Nonlinear flow behavior at low Reynolds numbers through rough-walled fractures subjected to normal compressive loading. Int J Rock Mech Min Sci 80:202–218

Zhou CB, Zhao XJ, Chen YF, Liao Z, Liu MM (2018) Interpretation of high pressure pack tests for design of impervious barriers under high-head conditions. Eng Geol 234:112–121

Zhu YWS, Zhang T (2018) Permeability of the coal seam floor rock mass in a deep mine based on in situ water injection tests. Mine Water Environ 37:724–733

Zimmerman RW, Bodvarsson GS (1996) Hydraulic conductivity of rock fractures. Transp Porous Media 23(1):1–30